Microporous and Mesoporous Materials 224 (2016) 392–399

Contents lists available at ScienceDirect

Microporous and Mesoporous Materials

journal homepage: www.elsevier.com/locate/micromeso

Adsorptive separation of C2/C3/C4-hydrocarbons on a flexible Cu-MOF: The influence of temperature, chain length and bonding character

Thomas Hähnel [a, *], Grit Kalies [a], Rajamani Krishna [b], Jens Möllmer [c], Jörg Hofmann [c], Merten Kobalz [d], Harald Krautscheid [d]

[a] HTW University of Applied Sciences, Chemical Engineering, Friedrich-List-Platz 1, D-01069, Dresden, Germany
[b] University of Amsterdam, Van't Hoff Institute for Molecular Sciences, Postbus 94157, 1090 GD Amsterdam, The Netherlands
[c] Institut für Nichtklassische Chemie eappsec1. (INC), 15 Permoserstrasse, D-04318, Leipzig, Germany
[d] Universität Leipzig, Institute of Inorganic Chemistry, 29 Johannisallee, D-04103, Leipzig, Germany

ARTICLE INFO

Article history:
Received 11 November 2015
Received in revised form
23 December 2015
Accepted 31 December 2015
Available online 9 January 2016

Keywords:
Adsorption isotherm
Flexible MOF
Stepwise adsorption
Phase transition
Hydrocarbon separation

ABSTRACT

In this work, manometrically and gravimetrically measured adsorption isotherms on the flexible copper MOF material $Cu_4(\mu_4\text{-}O)(\mu_2\text{-}OH)_2(Me_2trzpba)_4$ (**1**) are presented and discussed. This includes nitrogen (N_2) adsorption at 77.3 K, carbon dioxide (CO_2) adsorption at 298.15 K (Supplementary Material) and the adsorption of the five hydrocarbons ethane, ethene, propane, n-butane and 1-butene at 273.15 K, 298.15 K and 323.15 K. Up to the saturation pressure, all isotherms show distinct inflection characteristics, that are relatable to structural transitions of the flexible solid. The number of inflections and the relative pressure at which the inflections manifest depend on the characteristics of the relevant adsorptive and on temperature. For the hydrocarbon adsorption isotherms, we studied the influence of i) measurement temperature, ii) bonding character, and iii) the chain length of the alkanes and alkenes. In addition, the origin of decreasing equilibrium pressure with increasing adsorbed volume in the nitrogen adsorption isotherms on the flexible MOF material **1** is discussed. Calculations using the Ideal Adsorbed Solution Theory (IAST), based on the unary isotherm fits, along with transient breakthrough simulations, are used to demonstrate that Cu-MOF **1** has the potential to separate 5-component ethane/ethene/propane/n-butane/1-butene mixtures to yield three different fractions with increasing carbon numbers.

1. Introduction

Metal-organic frameworks (MOFs) as microporous materials with high adsorption capacity represent a challenge for the search of applications in many processes such as gas storage, separation or purification [1,2]. Frameworks of the third generation, according to the classification of Kitagawa et al., possess a more or less high degree of flexibility [3] that can depend on the solid structure itself, the fluid pressure and/or the loading with guest molecules – a special feature that may be exploited to find useful applications.

Fluid-dependent adsorption connected with definite solid–solid phase transitions, for instance, may be used for noble gas or hydrocarbon separation [4,5]. Since ethane and ethene possess very similar boiling points and molecular dimensions, mixtures of ethane/ethene are difficult to separate by distillation or molecular sieving. Therefore, energy-intensive processes such as cryogenic distillation are widely used for industrial ethane/ethene separation [6–8] which is important for feedstock purification in polyethene manufacture. In order to find a suitable adsorbent for ethane/ethene separation, Mofarahi et al. examined the usability of 5A zeolite. According to their simulations, 5A zeolite can be applied for separation of ethane/ethene by means of pressure swing adsorption (PSA) [9]. Different MOF materials have been investigated via olefin and paraffin adsorption, too. Martins et al. found that Cu-BTC has a distinct higher adsorption capacity for hydrocarbons than NaX and zeolite 13X [10]. In that work, the Cu-BTC shows a slightly higher adsorption affinity for ethene than for

* Corresponding author. HTW Dresden University of Applied Sciences, Department of Chemical Engineering, Friedrich-List-Platz 1, D-01069 Dresden, Germany. Tel.: +49 351 462 3880; fax: +49 0351 462 2177.
E-mail address: haehnel@htw-dresden.de (T. Hähnel).

http://dx.doi.org/10.1016/j.micromeso.2015.12.056
1387-1811/

ethane. It is assumed that, additionally to the smaller kinetic diameter, the higher quadrupole moment of ethene may be a reason for this finding. However, a possible π-bonding-interaction of ethene with the open metal sites of the framework is discussed as the main reason. Neutron powder diffraction experiments on the Fe-MOF Fe_2(dobdc) support this thesis [11]. A further plausible influencing factor is the binding of the hydrocarbons with framework oxygens due to the convenient conformation of ethene molecules compared with ethane molecules, which was simulated by Nicholson [12]. By means of transient breakthrough experiments, Gücüyener et al. [13] have demonstrated the separation of ethene/ethane mixtures using zeolitic imidazolate framework material (ZIF 7). In this case, ethane is preferentially adsorbed from the mixture; the selectivity has been attributed to gate opening mechanism and subtle differences in molecular configurations.

The Cu-MOF $Cu_4(\mu_4\text{-}O)(\mu_2\text{-}OH)_2(Me_2trzpba)_4$ (**1**, $Me_2trzpba^-$ = 4-(3,5-dimethyl-4H-1,2,4-triazol-4-yl)benzoate) investigated in this work, has been examined already in earlier studies [14–16]. Lincke et al. [14] described the synthesis of the material and found two distinct steps in the adsorption isotherms of N_2, Ar and CO_2 which are explained by gate-opening processes. Reichenbach et al. [15] proved the influence of handling and storage of the material on textural properties and showed that external stimuli, like temperature- and pressure gradients, can change the sorption characteristics and the degree of flexibility. Lange et al. [16] studied the adsorption behavior of n-butane, 1-butene, isobutane and isobutene on the Cu-MOF **1**.

The present communication has two major objectives. The first objective is to investigate systematically how measurement temperature, chain-length and bonding character influence the adsorption of alkanes and alkenes on the flexible Cu-MOF. The second objective is to demonstrate its potential for separation of hydrocarbon mixtures containing C2, C3, and C4 hydrocarbons; such separations are of importance in the petrochemical industries [17,18]. Published research on MOFs for the separation of mixtures of C4 hydrocarbons is extremely limited. For example, Hartmann et al. [19] have presented breakthrough experimental data to demonstrate the separation of isobutane/isobutene mixtures using CuBTC.

2. Experimental

2.1. Adsorbent

The Cu-MOF **1** was prepared using the synthesis route given by Lincke et al. [14]. The protonated ligand H(Me_2trzpba) was refluxed with copper acetate hydrate for two days in ethanol, followed by a Soxhlet extraction of the obtained material with methanol.

According to the single crystal structure analysis [14], the nodes of the framework are composed of four copper ions, each showing N_2O_3 pyramidal coordination sphere. A central O^{2-} ion represents the common vertex of the four pyramids and is therefore the central assemblage point surrounded by the four copper ions. Additionally, pairs of copper ions are bridged with each other either via bidentately binding triazole units or via hydroxyl groups. A body centered cubic topology is built up by connection of $Cu_4(\mu_4\text{-}O)(\mu_2\text{-}OH)_2$ nodes via organic linkers which leads to a three-dimensional pore system consisting of two different types of windows. Their dimensions are 450 × 550 pm in crystallographic *a* and *b* directions and 350 × 850 pm in *c* direction presented in Fig. 1 [14].

The MOF material was stored in methanol. Before activation, excessive solvent was decanted, and the material was first dried at 373.15 K for about 30 min, the pre-dried solid then was stored in methanol vapor in a desiccator.

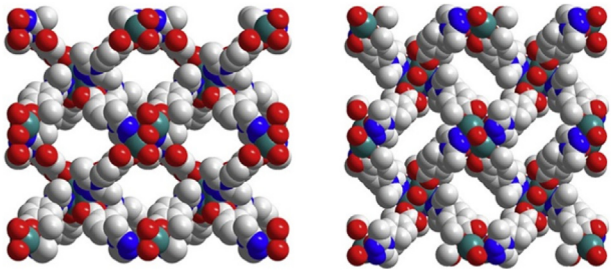

Fig. 1. Projections of the crystal structure of **1** which forms a three-dimensional pore system; view in crystallographic a and b directions 450 × 550 pm (left), c direction 350 × 850 pm (right) [14].

2.2. Manometric and gravimetric adsorption measurements

N_2 adsorption isotherms were measured at 77.3 K with a manometric ASAP 2010 device (Micromeritics Instrument Corporation) [20]. About 200 mg of the pre-dried substance were activated and weighed before the measurement. In order to avoid contact with atmospheric gases, a seal frit was used to cap the sample tube. For minimizing the sample tube volume during the manometric measurement, a filler rod was used. Defined volume increments were dosed automatically until the targeted relative pressures were reached.

Hydrocarbon adsorption isotherms at 273.15 K, 298.15 K and 323.15 K and the CO_2 adsorption isotherm at 298.15 K were measured with a magnetic suspension balance (Fa. Rubotherm) [21]. The pre-dried material was filled in a sample holder and brought into the vacuum system of the balance. Different pressure transducers were used depending on the expected pressure ranges of the measurement fluids. The saturation pressures of the used hydrocarbons at different temperatures are listed in Table 1.

After activation, the fluids were dosed stepwise to the measurement system. The adsorption equilibrium was monitored manually. Before changing the measurement fluid, the balance system was purged with the new fluid several times in order to remove remaining molecules from the previous adsorption experiment. The resulting sorption isotherms were corrected via helium buoyancy correction as discussed in Ref. [23].

3. Results and discussion

3.1. Nitrogen adsorption isotherm

We measured manometrically the N_2 adsorption isotherms on the Cu-MOF several times. We were able to reproduce the isotherms already published in Refs. [14] and [15] for the same material which show two strong increases (steps) of the adsorbed volume above a relative pressure of 10^{-3}. The second strong increase is associated with a large hysteresis loop. It is well-known

Table 1
Saturation pressures of the used adsorptives at all measured temperatures; calculated using a correlation provided by the Design Institute for Physical Properties (DIPPR) [22].

Adsorptive	Saturation pressure [bar]		
	273.15 K	298.15 K	323.15 K
ethane	23.9	41.9	68.6
ethene	41.1	69.8	111.7
propane	4.8	9.5	17.2
n-butane	1.0	2.4	5.0
1-butene	1.3	3.0	5.9

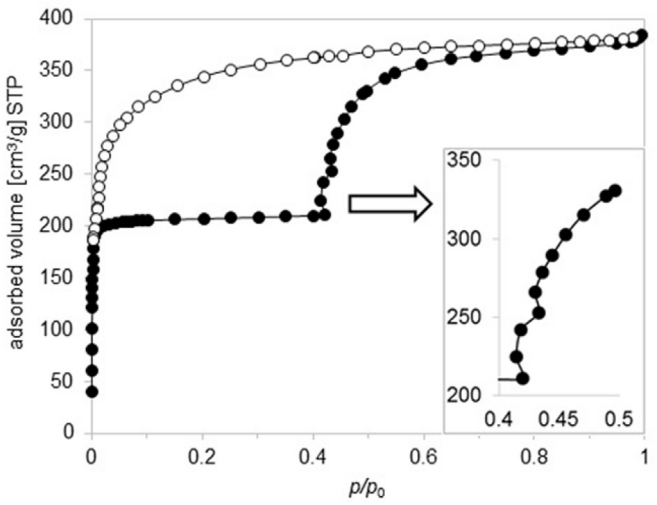

Fig. 2. Detailed presentation of N_2 physisorption at 77.3 K on **1**; adsorption: filled symbols, desorption: empty symbols.

that isotherms like that can be caused by structural transitions of the adsorbent, which has been discussed already for several flexible MOF-materials [3,24,25].

In order to have a closer look on the second step, a selected isotherm is presented in Fig. 2. It can be seen that at a relative pressure, $p/p_0 \approx 0.40–0.45$, negative rises in the isotherm shape can occur, i.e., the relative pressure decreases with an increasing amount of the adsorbed volume.

Since the effect of decreasing equilibrium pressure with increasing adsorbed amount was reproducible for different adsorption isotherms of the same MOF sample, it can be assumed that it is due to the flexibility of the material. In Fig. 3, we present a possible explanation for the occurrence of decreasing relative pressures with increasing amounts of the adsorbed volume.

During an adsorption experiment, constant amounts of measuring gas are dosed according to a defined pressure table. At each point, the adsorption equilibrium is awaited. In the following, we will consider two successive dosing steps after reaching $p/p_0 \approx 0.4$.

First dosing

At $p/p_0 = 0.4$, a limited part of the total pore quantity of the adsorbent is accessible for the adsorptive molecules. If now further adsorptive molecules (blue) are dosed into the system, during the equilibration, the original dosing pressure before adsorption decreases down to the equilibrium pressure. This equilibrium pressure is higher than the previous equilibrium value of $p/p_0 = 0.4$ because the gate-opening pressure is not yet reached.

Second dosing

After the dosing of new adsorptive molecules (red), together with the residual non-adsorbed gas molecules (blue) of the first adsorption equilibrium, a higher dosing pressure than at the first dosing is reached. If the second dosing pressure is now higher than the gate-opening pressure, additional pore regions become accessible for the measurement gas. Both the residual molecules (blue) as well as the new molecules (red) will be adsorbed in the whole open pore system. If the capacity of the additional pore system is large enough, then the equilibrium pressure after the second step is smaller than the equilibrium pressure of the first dosing.

So, the flexible behavior of the solid may lead to a decreasing equilibrium pressure with increasing adsorbed amount in the adsorption isotherm. The effect can be explained by reaching of the gate-opening pressure between two dosing steps before reaching the adsorption equilibrium. Related phenomena were for example discussed by Tanaka et al. [26] or Tezel et al. [27] and have been reproduced and even deepened by recent micro-imaging studies by which the evolution of the guest-induced changes in the lattice structure could be recorded in time dependent maps of the crystal [28].

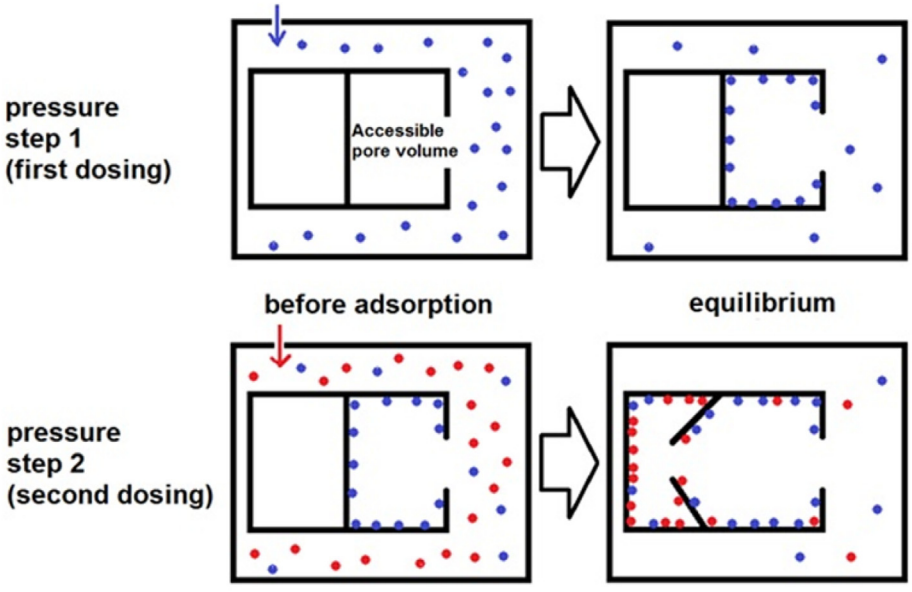

Fig. 3. Assumed process leading to the effect of decreasing equilibrium pressure with increasing adsorbed amount in physisorption isotherms.

3.2. Hydrocarbon adsorption isotherms

The isotherms of the five light hydrocarbons ethane, ethene, propane, n-butane and 1-butene were measured at 273.15 K, 289.15 K and 323.15 K. In the following, we will present selected isotherms by emphasizing the parameters temperature, chain length and bonding character influencing the adsorption behavior of the Cu-MOF material.

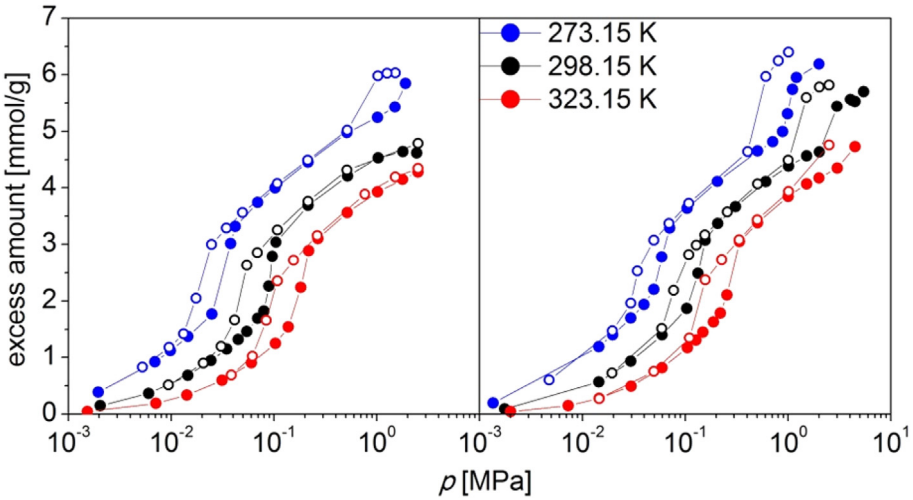

Fig. 4. Semi-logarithmic presentation of the ethane (left) and ethene (right) isotherms on **1** at 273.15 K, 298.15 K and 323.15 K; adsorption: filled symbols, desorption: empty symbols.

3.2.1. Influence of temperature and bonding character of the hydrocarbons

In Fig. 4, the gravimetrically measured isotherms of ethane and ethene are presented. It can be seen that all isotherms show hysteresis associated with strong increases of the excess amount with increasing pressure, subsequently designated as isotherm steps. The number of hysteresis and the respective isotherm steps depends on temperature and the respective fluid adsorptive.

If one compares the ethane isotherms on the left-hand side of Fig. 4 with the ethene isotherms on the right-hand side, it becomes obvious that more or less all ethene isotherms are two-step isotherms, whereas for the ethane adsorption at 298.15 K and 323.15 K, also one-step isotherms can be found. This indicates two solid–solid phase transitions due to ethene adsorption of the Cu-MOF **1** in the measured pressure range at all measured temperatures. Ethane adsorption leads to this behavior only at 273.15 K. This indicates that the bonding character of the respective hydrocarbon may influence the gate-opening process.

Due to the π-bonding of ethene, the two hydrocarbons ethane and ethene differ in the following properties which might affect the shape of the adsorption isotherms:

1 the π-bonding character of ethene which possibly influences the coordinative properties of the adsorbent,
2 the smaller kinetic diameter of ethene compared with ethane molecules providing better accessibility of ethene to the pores of the microporous framework (steric effects),
3 the higher saturation pressure of ethene compared with ethane, which may lead to a higher stress on the inner framework and therefore a supported solid–solid phase transition.

However, it can be assumed that a more or less complex interplay between the mentioned influences leads to the respective behavior of the adsorbent.

As expected, the position of the steps in the isotherms of both adsorptives is shifted to higher pressures with increasing temperature. In each isotherm, the first step starts if nearly the same values of excess amount are reached. This suggests that the beginning of the solid–solid phase transition is related to a certain degree of surface coverage. However, the excess amount of gate opening decreases slightly with increasing temperature. This may be explained by the higher kinetic energy of the adsorbate molecules at higher temperatures.

For ethene, the first steps start at slightly higher excess amounts than for ethane, which may be explained by the covered surface area. In order to cover the same surface area, a larger amount of ethene molecules is needed than of ethane molecules because of the smaller kinetic diameter of the ethene molecules. The ranges of excess amounts, where isotherm steps occur, are listed for all measured temperatures and all adsorptives in Table 2.

In Fig. 5, for a more detailed discussion, the adsorption isotherms of ethane and ethene are overlapped for each measured temperature. For all temperatures, in the low relative pressure region, the ethane and ethene isotherms are very similar. Visible differences between the ethane and ethene isotherms can be observed only in the region of the first adsorption hysteresis at $p/p_0 \approx 10^{-2}$. Finally, the differences between the isotherms are small up to $p/p_0 = 10^{-1}$.

Significant differences between the isotherms at the respective temperature, however, can be found for $p/p_0 > 10^{-1}$ as already mentioned in the discussion of Fig. 4.

For 273.15 K, both isotherms show a second step which occurs for ethene at a lower relative pressure than for ethane. At the higher temperatures 298.15 K and 323.15 K, a second isotherm step is only seen for ethene. That confirms the theory, that the second phase transition of the Cu-MOF **1** is supported by the bonding character of the hydrocarbons and the related properties of the adsorptives.

Table 2
Ranges of excess amounts $\Delta\Gamma$ related to isotherm steps.

Transition steps	Temperature	Ethane	Ethene	Propane	n-butane	1-butene
		$\Delta\Gamma$ [mmol/g]	$\Delta\Gamma$ [mmol/g]	$\Delta\Gamma$ [mmol/g]	$\Delta\Gamma$ [mmol/g]	$\Delta\Gamma$ [mmol/g]
1st step [mmol/g]	273.15 K	1.8–3.3	2.2–3.4	1.2–2.9	1.1–2.2	1.4–2.4
	298.15 K	1.8–3.0	1.9–3.0	1.0–3.3	1.1–2.1	1.3–2.4
	323.15 K	1.5–2.9	1.8–3.1	0.9–2.6	1.0–2.1	1.3–2.0

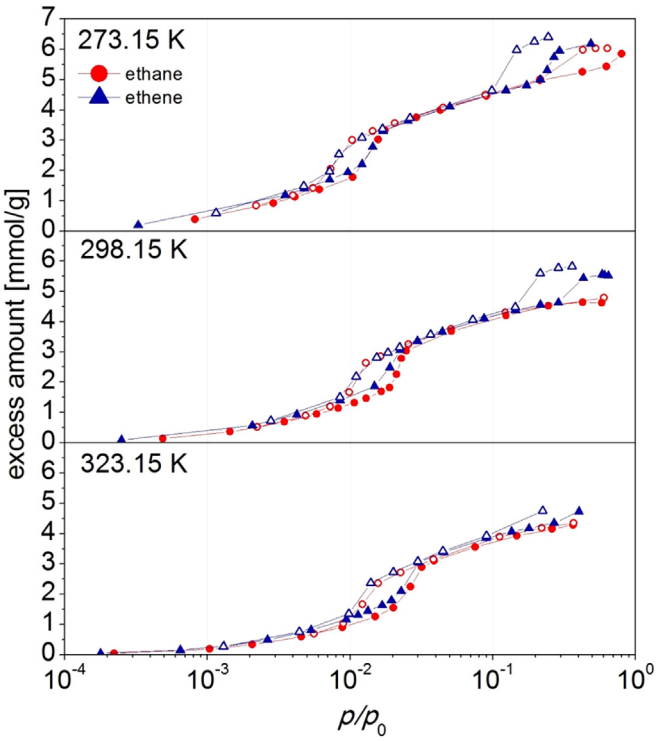

Fig. 5. Semi-logarithmic presentation of the ethane (red) and ethene (blue) isotherms on **1** at 273.15 K, 298.15 K and 323.15 K; adsorption: filled symbols, desorption: empty symbols. (For interpretation of the references to colour in this figure legend, the reader is referred to the web version of this article.)

3.2.2. *Influence of chain-length and temperature*

In Fig. 6, the measured ethane and propane adsorption isotherms are compared. At all temperatures, a stepwise isotherm progression is apparent. The steps are combined again with hysteresis loops. While the ethane isotherms on the left-hand side show one- and two-step isotherms (cf. also Fig. 4), the propane isotherms show a one-step progression for all temperatures. This suggests that the flexible behavior of the framework is provided with decreasing chain length of the adsorbed molecules.

3.2.3. *Influence of chain-length and bonding character of the hydrocarbons*

Fig. 7 shows the adsorption of three saturated hydrocarbons (left-hand side) and of two unsaturated hydrocarbons (right-hand side) at 273.15 K. All isotherms show a stepwise curve progression. Propane and n-butane show one-step isotherms and ethane, ethene and 1-butene show two-step ones. It can be seen that in case of saturated hydrocarbon adsorption, the adsorptive chain length influences the flexible behavior of the Cu-MOF material. In case of the adsorption of unsaturated hydrocarbons, this influence is not so obvious. For ethene as well as 1-butene, two-step isotherms are found.

In the initial relative pressure range of all isotherms, the excess amount increases with decreasing saturation pressure of pure adsorptive gas (see also Table 1). With increasing relative pressure the trend changes. Here, instead of saturation pressure the chain length of the adsorbed molecules is the main influencing factor. The excess amount increases with decreasing chain length of the adsorbed molecules. This is due to the fact that in a constant pore volume, larger amounts of small molecules than of larger ones are adsorbable.

The influence of the bonding character of adsorbed molecules becomes obvious by comparing the n-butane and 1-butene isotherms at 273.15 K (see Fig. 8). The second step in the 1-butene isotherm gives evidence that the flexible behavior of **1** is provided, if π-bonding interactions between adsorbate molecules and the adsorbent take place. Maybe this is due to a supported change of metal site coordination in the Cu-MOF **1** [10,11]. Also influences due to the smaller kinetic diameter or the higher saturation pressure of the unsaturated hydrocarbon compared with the saturated one of the same chain length may play a role. Lange et al. [16] carried out in-situ-PXRD measurements and showed that only 1-butene-adsorption causes a second gate-opening step. The adsorption isotherms of other C_4-hydrocarbons such as isobutane and isobutene showed only one distinct increase, i.e. the influence of the conformation and the π-bonding of adsorptive molecules in the adsorption behavior has been demonstrated.

In Table 2, the ranges of excess amounts related to isotherm steps are presented for all measured adsorptives and temperatures. It can be seen that the kind of adsorbed substance influences the range of the excess amount stronger than the measurement temperature. For the C_2-hydrocarbons, the ranges of excess amounts related to isotherm steps start at higher values than for propane

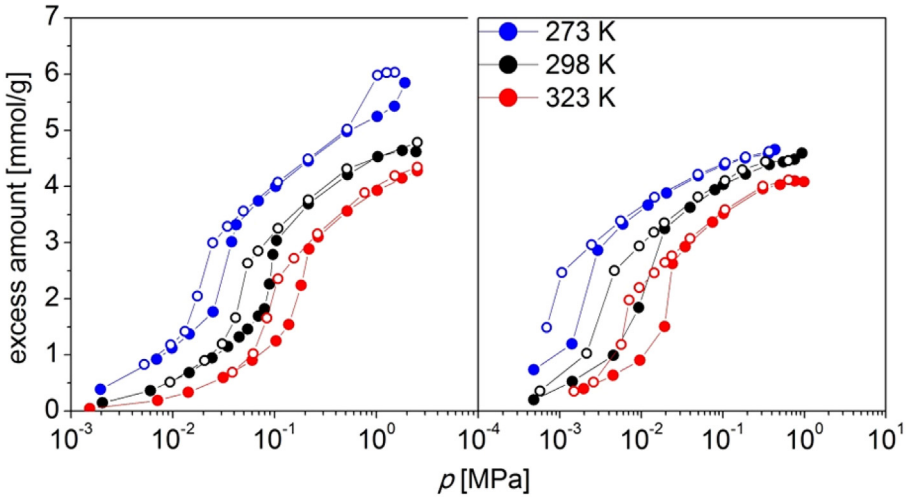

Fig. 6. Semi-logarithmic presentation of the ethane (left) and propane (right) isotherms on **1** at 273.15 K, 298.15 K and 323.15 K; adsorption: filled symbols, desorption: empty symbols.

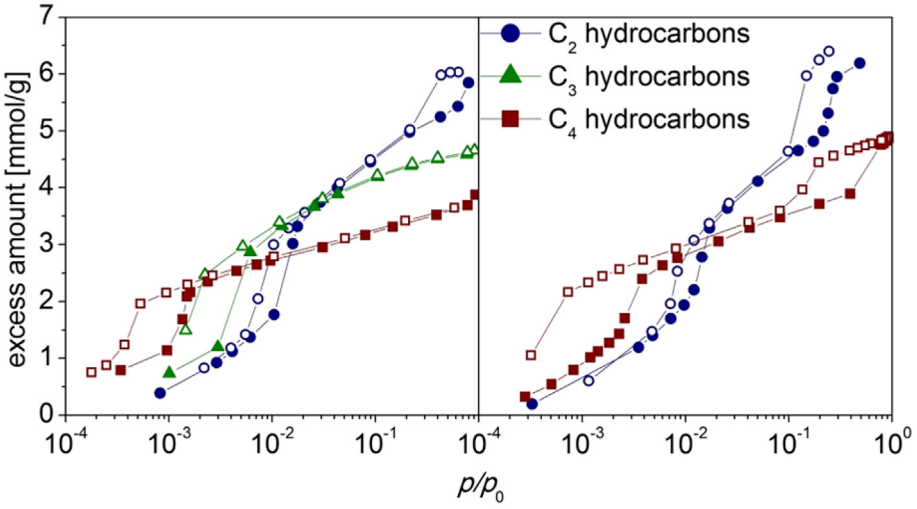

Fig. 7. Semi-logarithmic presentation of isotherms with saturated hydrocarbons (left) and unsaturated hydrocarbons (right) on **1** at 273.15 K; adsorption: filled symbols, desorption: empty symbols.

and C_4-hydrocarbons – probably an effect of the space filling requirements of the different adsorptive molecules. A larger amount of small molecules is needed to cover the same surface areas for starting a structural transition. It is also obvious that the excess amounts for unsaturated hydrocarbons are slightly higher than for the saturated ones of the same chain length.

For a more quantitative evaluation of the occurring solid state phases of the Cu-MOF **1** (P1, P2, P3), cumulative pore volumes were calculated using the Gurvich rule [29,30]. In Table 3, the calculated values for all measured adsorptives and temperatures are listed. The values are percentages referred to the theoretical pore volume of 0.59 cm^3/g from Ref. [14]. No data are listed if no phase transition occurred or if the measurement fluid is supercritical at the corresponding temperature. Independent of the used adsorptive or temperature, comparable pore volumes are calculated for each of the three phases. Phase 1, existing under low pressure conditions, offers an average pore volume of about 21%, phase 2 of about 65% and phase 3 of about 83% of the complete theoretical pore volume.

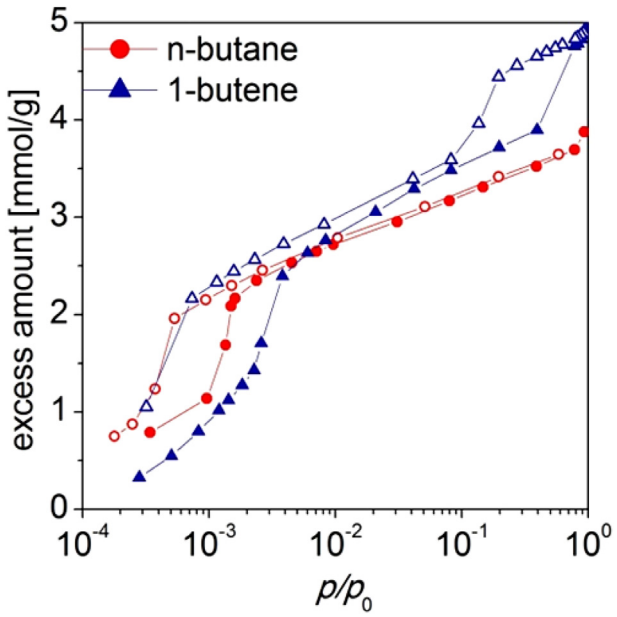

Fig. 8. Semi-logarithmic presentation of the n-butane (red) and 1-butene (blue) isotherms on **1** at 273.15 K adsorption: filled symbols, desorption: empty symbols. (For interpretation of the references to colour in this figure legend, the reader is referred to the web version of this article.)

4. The potential of Cu-MOF 1 for C2/C3/C4-mixture separations

In order to investigate the separation potential of **1**, the Ideal Adsorbed Solution Theory (IAST) was applied to determine the component loadings in equilibrium with equimolar 5-component ethane/ethene/propane/n-butane/1-butene mixtures. For performing the IAST calculations, the unary isotherms of each guest molecule are fitted with good accuracy using the three-site Langmuir–Freundlich model; details of the isotherm fits, along with IAST calculations are provided in the Supplementary Material available in the online version of this article. At 298 K, for example, IAST calculations of the component loadings in the adsorbed phase are shown in Fig. 9. We also note that component loadings are bunched into three fractions: C4-, C3- and C2-hydrocarbons. This indicates that ethene/ethane/propane/n-butane/1-butene gas mixtures can be separated into three fractions with different carbon numbers.

Industrial separations of hydrocarbon mixtures are normally carried out in fixed bed adsorption devices. The performance of a

Table 3
Cumulative pore volumes of different occurring solid state phases and at different temperatures, calculated by the Gurvich rule; percentage presentation, referred to the theoretical pore volume of 0.59 cm^3/g.

	Calculated pore volume [%]				
	ethane	ethene	propane	n-butane	1-butene
273.15 K/P1	22.5	30.8	17.0	18.7	24.0
273.15 K/P2	69.7	70.0	66.0	60.5	65.3
273.15 K/P3	77.4	87.1	–	–	83.1
298.15 K/P1	29.6	–	15.0	19.3	22.0
298.15 K/P2	75.9	–	68.3	59.2	65.0
298.15 K/P3	–	–	–	–	–
323.15 K/P1	–	–	15.0	18.7	22.9
323.15 K/P2	–	–	68.6	57.4	62.5
323.15 K/P3	–	–	–	–	–

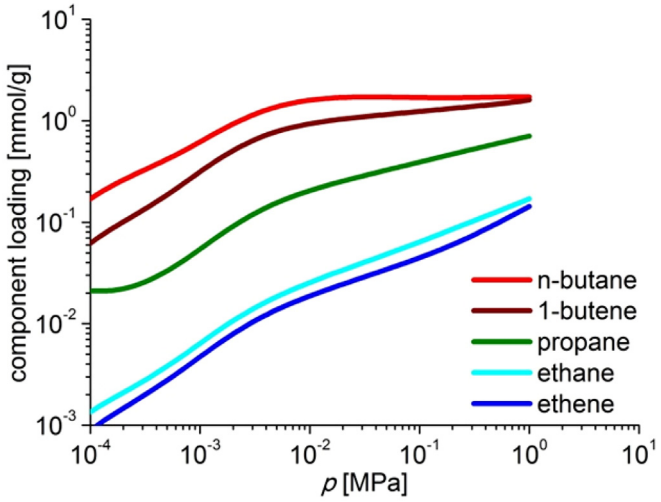

Fig. 9. IAST calculations of component loadings for adsorption of 5-component ethane/ethene/propane/n-butane/1-butene mixtures (equimolary: y = 0.20) in **1** maintained at 298 K.

fixed bed adsorber is dictated by a combination of adsorption selectivity and uptake capacity. To examine the separation potential of **1**, transient breakthrough simulations are performed using the methodology described in earlier work [18]. For operation of a fixed bed adsorber at 298 K, and total pressure of 5 bar, the transient breakthroughs are shown in Fig. 10. The elution sequence is ethene, ethane, propane, 1-butene, and n-butane. For appreciation of the breakthroughs, a video animation of the transient traversal of the gas phase concentration fronts of each of the five guest molecules along the length of the fixed bed has been uploaded as supplementary material. The breakthroughs suggest that the exit gas can be collected in three separate fractions with different C numbers, as indicated by the arrows in Fig. 10. Further experimentation is necessary in order to confirm this promising separation potential for industrially relevant operation conditions.

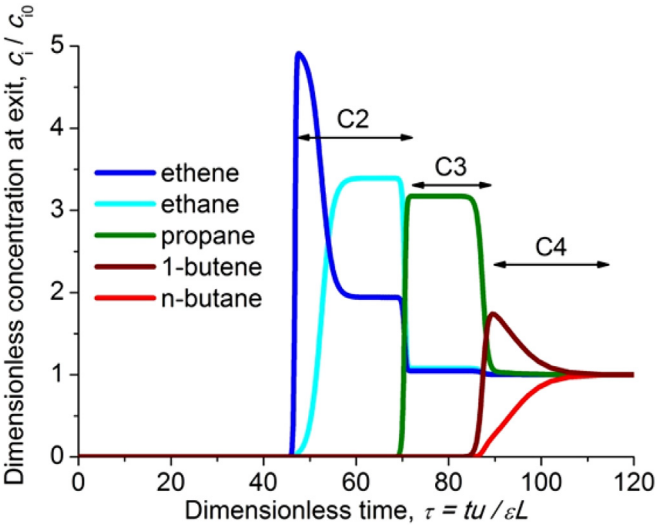

Fig. 10. Simulations of transient breakthrough characteristics for 5-component ethane/ethene/propane/n-butane/1-butene gas mixtures in Cu-MOF **1** maintained at isothermal conditions at 298 K. The partial pressure of each component in the inlet gas to the fixed bed is 1 bar.

Supplementary data related to this article can be found online at http://dx.doi.org/10.1016/j.micromeso.2015.12.056.

5. Conclusions

Experimental adsorption on the flexible copper MOF material **1** of nitrogen at 77.3 K and the five hydrocarbons ethane, ethene, propane, n-butane and 1-butene at 273.15 K, 298.15 K and 323.15 K have been presented and discussed.

The main results of the experimental investigations are:

1. Concerning nitrogen adsorption isotherms, we suggest a mechanism by which the unusual behavior of increasing adsorbed amount with decreasing equilibrium pressure may be explained by the flexible behavior of the adsorbent material.
2. All isotherms show more or less distinct steps, which can be related to structural transitions of the flexible solid.
3 The lower the measurement temperature the higher is the excess amount of the respective hydrocarbon. At 273.15 K, two-step isotherms can be expected with higher probability than at the higher temperatures of 298.15 K and 323.15 K since the adsorption forces at 273.15 K are strong enough to open the pore system of the flexible material. At 273.15 K, we found two-step isotherms for ethane, ethene and 1-butene. At 298.15 K and 323.15 K, two-step isotherms only occur for ethene in the measured relative pressure range. However, at the higher temperatures the experimental setup limits the reachability of the maximum relative pressures.
4 For the unsaturated hydrocarbons, more two-step isotherms have been found than for the respective saturated hydrocarbons of the same chain length. This indicates that the bonding character of the adsorptive molecules influences the flexible behavior of the Cu-MOF **1.** This is maybe due to π-bonding interactions with the adsorbent, the kinetic diameter or the differing saturation pressure of the adsorptives.
5 The lower the chain length of the respective adsorptive the more the flexible behavior of the adsorbent is provided. In the higher relative pressure region, the excess amount increased with decreasing chain length. This applies to the unsaturated as well as the saturated hydrocarbons.

The following conclusions can be drawn from the simulated data (cf. also supplementary Material):

1. Cu-MOF **1** has the potential to separate C2/C3/C4 hydrocarbon mixtures to yield three different fractions with different C numbers. For clean separation between the C3 and C4 fractions, the operating temperatures need to be within 298 K and 323 K.
2. IAST calculations show that ethane/ethene mixtures cannot be separated effectively by Cu-MOF **1.**
3. Cu-MOF **1** is capable of separating n-butane/1-butene mixtures to yield pure 1-butene, provided the temperature is maintained at 273 K. The gate opening is less selective for this separation at higher temperatures of 298 K and 323 K.

Acknowledgment

The financial support for this project by Deutsche Forschungsgemeinschaft (DFG, KA-1560/6-1) and Bundesministerium für Bildung und Forschung (BMBF, 03FH041PX4) is gratefully acknowledged.

We also want to express our thanks to Marcus Lange (INC Leipzig) who supported the gravimetric adsorption measurements and Sebastian Storch (HTW Dresden) who carried out the manometric N_2 adsorption on the Cu-MOF material.

Appendix A. Supplementary data

Supplementary data related to this article can be found at http://dx.doi.org/10.1016/j.micromeso.2015.12.056.

Notation

c_i	molar concentration of species i in gas mixture, mol/m^3
c_{i0}	molar concentration of species i in gas mixture at inlet to adsorber, mol/m^3
L	length of packed bed adsorber, m
p	total system pressure, MPa
p/p_0	relative pressure
t	time, s
T	absolute temperature, K
u	superficial gas velocity in packed bed, m/s
y	mole fraction of hydrocarbons in equimolary mixture

Greek letters

ε	voidage of packed bed, dimensionless
$\Delta\Gamma$	ranges of excess amounts related to isotherm steps, mmol/g
τ	time, dimensionless

Abbreviations

P1/P2/P3 occurring solid state phases (1, 2, 3) of Cu-MOF **1** during adsorption experiments

References

[1] A. Czaja, N. Trukhan, U. Müller, Chem. Soc. Rev. 38 (2009) 1284–1293.
[2] R. Kuppler, D. Timmons, Q.-R. Fang, J.-R. Li, T. Makal, M. Young, D. Yuan, D. Zhao, W. Zhuang, H.-C. Zhou, Coord. Chem. Rev. 253 (2009) 3042–3066.
[3] S. Kitagawa, U. Kazuhiro, Chem. Soc. Rev. 34 (2005) 109–119.
[4] Z. Herm, E. Bloch, J. Long, Chem. Mater. 26 (2014) 323–338.
[5] J. Perry, S. Teich-McGoldrick, S. Meek, J. Greathouse, M. Haranczyk, M. Allendorf, J. Phys. Chem. C. 118 (2014) 11685–11698.
[6] R. Eldridge, Ind. Eng. Chem. Res. 32 (1993) 2208–2212.
[7] J.-R. Li, J. Sculley, H.-C. Zhou, Chem. Rev. 112 (2012) 869–932.
[8] J. Ploegmakers, A. Jelsma, A. van der Ham, K. Nijmeijer, Ind. Eng. Chem. Res. 52 (2013) 6524–6539.
[9] M. Mofarahi, S. Salehi, Adsorption 19 (2013) 101–110.
[10] V. Martins, A. Ribeiro, A. Ferreira, U.-H. Lee, Y. Hwang, J.-S. Chang, J. Lourero, A. Rodrigues, Sep. Purif. Technol. 149 (2015) 445–456.
[11] E. Bloch, W. Queen, R. Krishna, J. Zadrozny, C. Brown, J. Long, Science 335 (2012) 1606–1610.
[12] T. Nicholson, S. Bhatia, J. Phys. Chem. B. 110 (2006) 24834–24836.
[13] C. Gücüyener, J. van den Bergh, J. Gascon, F. Kapteijn, J. Am. Chem. Soc. 132 (2010) 17704–17706.
[14] J. Lincke, D. Lässig, J. Moellmer, C. Reichenbach, A. Puls, A. Moeller, A. Gläser, G. Kalies, R. Staudt, H. Krautscheid, Microporous Mesoporous Mater. 142 (2011) 62–69.
[15] C. Reichenbach, G. Kalies, J. Lincke, D. Lässig, H. Krautscheid, J. Moellmer, M. Thommes, Microporous Mesoporous Mater. 142 (2011) 592–600.
[16] M. Lange, M. Kobalz, J. Bergmann, D. Lässig, J. Lincke, J. Möllmer, A. Möller, J. Hofmann, H. Krautscheid, R. Staudt, R. Gläser, J. Mater. Chem. A. 2 (2014) 8075–8085.
[17] R. Krishna, Phys. Chem. Chem. Phys. 17 (2015) 39–59.
[18] R. Krishna, RSC Adv. 5 (2015) 52269–52295.
[19] M. Hartmann, S. Kunz, D. Himsl, O. Tangermann, S. Ernst, A. Wagener, Langmuir 24 (2008) 8634–8642.
[20] Micromeritics Instrument Corporation, ASAP 2010-Accelerated Surface Area and Porosimetry System – Operator's Manual V1.01, 1994.
[21] F. Dreisbach, A. Reza Seif, H. Lösch, Chem. Ing. Tech. 74 (2002) 1353–1366.
[22] T. Daubert, R. Danner, Physical and Thermodynamic Properties of Pure Chemicals: Data Compilation, Hemisphere, New York, 2003.
[23] J. Möllmer, A. Möller, F. Dreisbach, R. Gläser, R. Staudt, Microporous Mesoporous Mater. 138 (2011) 140–148.
[24] A. Boutin, F.-X. Coudert, M.-A. Springuel-Huet, A. Neimark, G. Ferey, A. Fuchs, J. Phys. Chem. 114 (2010) 22237–22244.
[25] A. Schneemann, V. Bon, I. Schwedler, I. Senkovska, S. Kaskel, R. Fischer, Chem. Soc. Rev. 43 (2014) 6062–6096.
[26] D. Tanaka, K. Nakagawa, M. Higuchi, S. Horike, Y. Kubota, T. Kobayaschi, M. Takata, S. Kitagawa, Angew. Chem. Int. Ed. 47 (2008) 3914–3918.
[27] O. Tezel, D. Ruthven, J. Colloid Interface Sci. 139 (1990) 581–583.
[28] J. Kärger, T. Binder, C. Chmelik, F. Hibbe, H. Krautscheid, R. Krishna, J. Weitkamp, Nat. Mater. 13 (2014) 333–343.
[29] L. Gurvich, J. Phys. Chem. Soc. Russ. 47 (1915) 805.
[30] S. Lowell, J. Shields, M. Thomas, M. Thommes, Characterization of Porous Solids and Powders: Surface Area, Pore Size and Density, Springer, Dordrecht, 2006.

Supplementary Material to accompany

Adsorptive separation of C2/C3/C4-hydrocarbons on a flexible Cu-MOF: The influence of temperature, chain length and bonding character

Thomas Hähnel[1], Grit Kalies[1], Rajamani Krishna[2], Jens Möllmer[3], Jörg Hofmann[3], Merten Kobalz[4], Harald Krautscheid[4]

[1] HTW University of Applied Sciences, Chemical Engineering, 1 Friedrich-List-Platz, D-01069, Dresden, Germany

[2] University of Amsterdam, Van't Hoff Institute for Molecular Sciences, Postbus 94157, 1090 GD Amsterdam, The Netherlands

[3] Institut für Nichtklassische Chemie e.V. (INC), 15 Permoserstrasse, D-04318, Leipzig, Germany

[4] Universität Leipzig, Institute of Inorganic Chemistry, 29 Johannisallee, D-04103, Leipzig, Germany

Author to whom correspondence should be sent:

Thomas Hähnel
HTW Dresden University of Applied Sciences
Department of Chemical Engineering
1 Friedrich-List-Platz
D-01069 Dresden
Phone: +49-351-462 3880
Fax: +49-0351-462 2177
E-mail: haehnel@htw-dresden.de

Table of Contents

1. Introduction

There has been considerable research on the development of MOFs for separation of light hydrocarbon mixtures containing two or more of the following components CH_4, C_2H_2, C_2H_4, C_2H_6, C_3H_6, and C_3H_8.[1-17] However, published research on MOFs for the separation of mixtures of C4 hydrocarbons is extremely limited. For example, Hartmann et al.[18] have presented breakthrough experimental data to demonstrate the separation of isobutane/isobutene mixtures using CuBTC. One of the objectives of this article is to examine the potential of $Cu_4(\mu4\text{-}O)(\mu2\text{-}OH)_2(Me_2trzpba)_4$ (= Cu-MOF **1**) for separation of mixtures containing C2-, C3- and C4-hydrocarbons, that are encountered say in cracker gases in petrochemical industries. The separation potential of the flexible Cu-MOF is established on the basis of measurements of pure component isotherms, IAST calculations of mixture adsorption equilibrium, and transient breakthrough simulations.

2. Characterization of Cu-MOF 1 by pure gas adsorption experiments

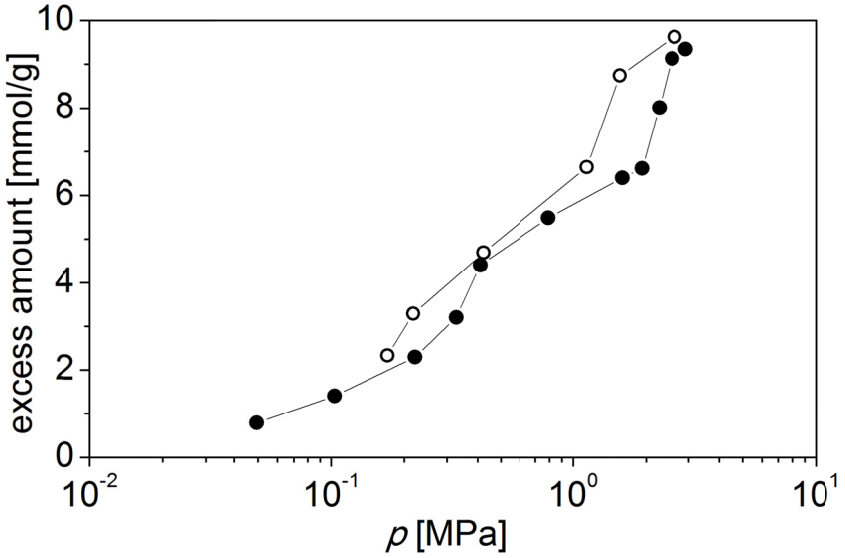

Fig. SM 1: Semi-logarithmic presentation of the CO_2 isotherm at 298.15 K on 1; adsorption: filled symbols, desorption: empty symbols.

Table SM 1: Used pressure transducers for gravimetric adsorption experiments with light hydrocarbons.

Pressure transducer	Manufacturer	Measurement range
MKS Baratron (0...10 mbar)	MKS Instruments GmbH	0...10 mbar
MKS Baratron (0...1 bar)	MKS Instruments GmbH	0...1 bar
PAA21-V-2.5	Omega Engineering Inc.	0...2.5 bar
PAA33X-V-30	Omega Engineering Inc.	0...30 bar
PAA21-V-50	Omega Engineering Inc.	0...50 bar
PAA21-V-160	Omega Engineering Inc.	0...160 bar

3. Fitting of experimental data on pure component isotherms

The experimentally determined *excess* isotherm loadings were converted to *absolute* loadings using

$$q = q^{excess} + \frac{pV_{pore}}{ZRT} \tag{1}$$

where Z is the compressibility factor. The Peng-Robinson equation of state was used to estimate Z. The accessible pore volume within the crystals, V_{pore}, was taken to be equal to experimentally determined value of 0.59 cm^3/g. The pure component isotherm data for ethene, ethane, propane, n-butane, and 1-butene display multiple inflections and a proper description of these is provided by the 3-site Langmuir-Freundlich model:

$$q = q_{A,sat}\frac{b_A p^{\nu_A}}{1+b_A p^{\nu_A}} + q_{B,sat}\frac{b_B p^{\nu_B}}{1+b_B p^{\nu_B}} + q_{C,sat}\frac{b_C p^{\nu_C}}{1+b_C p^{\nu_C}} \tag{2}$$

with T-dependent parameters b_{A}, b_{B}, and b_{C}

$$b_A = b_{A0}\exp\left(\frac{E_A}{RT}\right); \quad b_B = b_{B0}\exp\left(\frac{E_B}{RT}\right); \quad b_C = b_{C0}\exp\left(\frac{E_C}{RT}\right) \tag{3}$$

The adsorption and desorption branches of the isotherms were fitted separately. The saturation capacities q_{sat}, Langmuir constants b, Energy parameters E, and the Freundlich exponents ν, for ethene, ethane, propane, n-butane, and 1-butene are provided in Table SM 1.

Table SM 2: 3-site Langmuir-Freundlich parameters for ethene, ethane, propane, 1-butene and n-butane in Cu-MOF 1. These fit parameters are for the adsorption branches of the isotherms at 273 K, 298 K, and 323 K fitted together.

Parameter	**ethene**	**ethane**	**propane**	**1-butene**	**n-butane**
$q_{A,sat}$ / mol kg^{-1}	3.8	0.55	3.7	34	1
$q_{B,sat}$ / mol kg^{-1}	4.5	35	0.82	3.4	2.6
$q_{C,sat}$ / mol kg^{-1}	0.5	4.8	0.95	0.13	0.4
b_{A0} / Pa$^{-\nu_{iA}}$	1.09×10^{-26}	1.06×10^{-10}	1.36×10^{-11}	3.32×10^{-17}	0.33×10^{-17}
b_{B0} / Pa$^{-\nu_{iB}}$	1.91×10^{-13}	9.12×10^{-16}	6.29×10^{-18}	5.02×10^{-10}	4.01×10^{-16}
b_{C0} / Pa$^{-\nu_{C}}$	1.16×10^{-11}	1.8×10^{-13}	1.37×10^{-8}	2.21×10^{-12}	2.52×10^{-12}
E_A/ kJ mol^{-1}	50.7	35.2	34	52.5	55
E_B/ kJ mol^{-1}	34	33.3	29	34.8	65
E_C/ kJ mol^{-1}	36.2	35.6	34	38.2	56
ν_A / dimensionless	2.6	1	1.23	1	1.24
ν_B / dimensionless	1.3	1.14	2	1	1.37
ν_C / dimensionless	1.2	1.27	0.42	3.3	1.33

Fig. SM 2 presents comparisons of experimental data for the adsorption branch of the unary isotherms for (a) ethene, (b) ethane, (c) propane, (d) n-butane, and (e) 1-butene at 273 K, 298 K and 323 K with the 3-site Langmuir-Freundlich model fits. The fits are of good accuracy at all three temperatures for every guest molecule. Similar good accuracy is observed for the fitting of the desorption branches of the curves with equation (2).

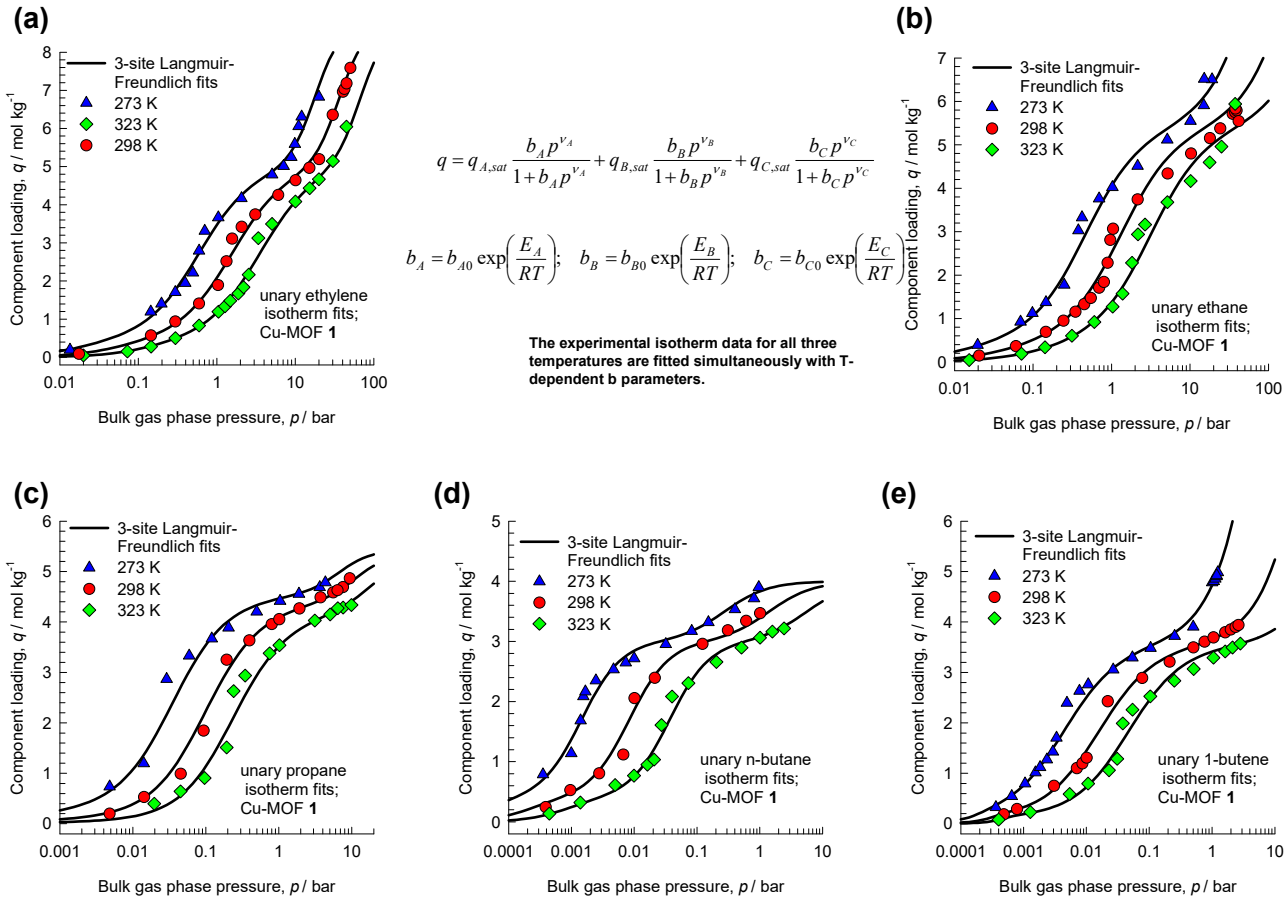

Fig. SM 2: Comparisons of experimental data for the adsorption branch of the unary isotherms for (a) ethene, (b) ethane, (c) propane, (d) n-butane, and (e) 1-butene at 273 K, 298 K and 323 K in Cu-MOF **1** with 3-site Langmuir-Freundlich model fits.

4. Isotherm inflections and the inverse thermodynamic factor

The inflections in the unary isotherms are best reflected in the calculations of the inverse thermodynamic factor, 1/Γ, defined by

$$\frac{1}{\Gamma} \equiv \frac{\partial \ln q}{\partial \ln p} = \frac{p}{q}\frac{\partial q}{\partial p} \tag{4}$$

The variation of 1/Γ with the component loading, q, can be determined by analytic differentiation of the 3-site Langmuir-Freundlich model fits. At any given temperature, for each molecule we observe two inflections, related to the structural transformations; see Fig. SM 3.

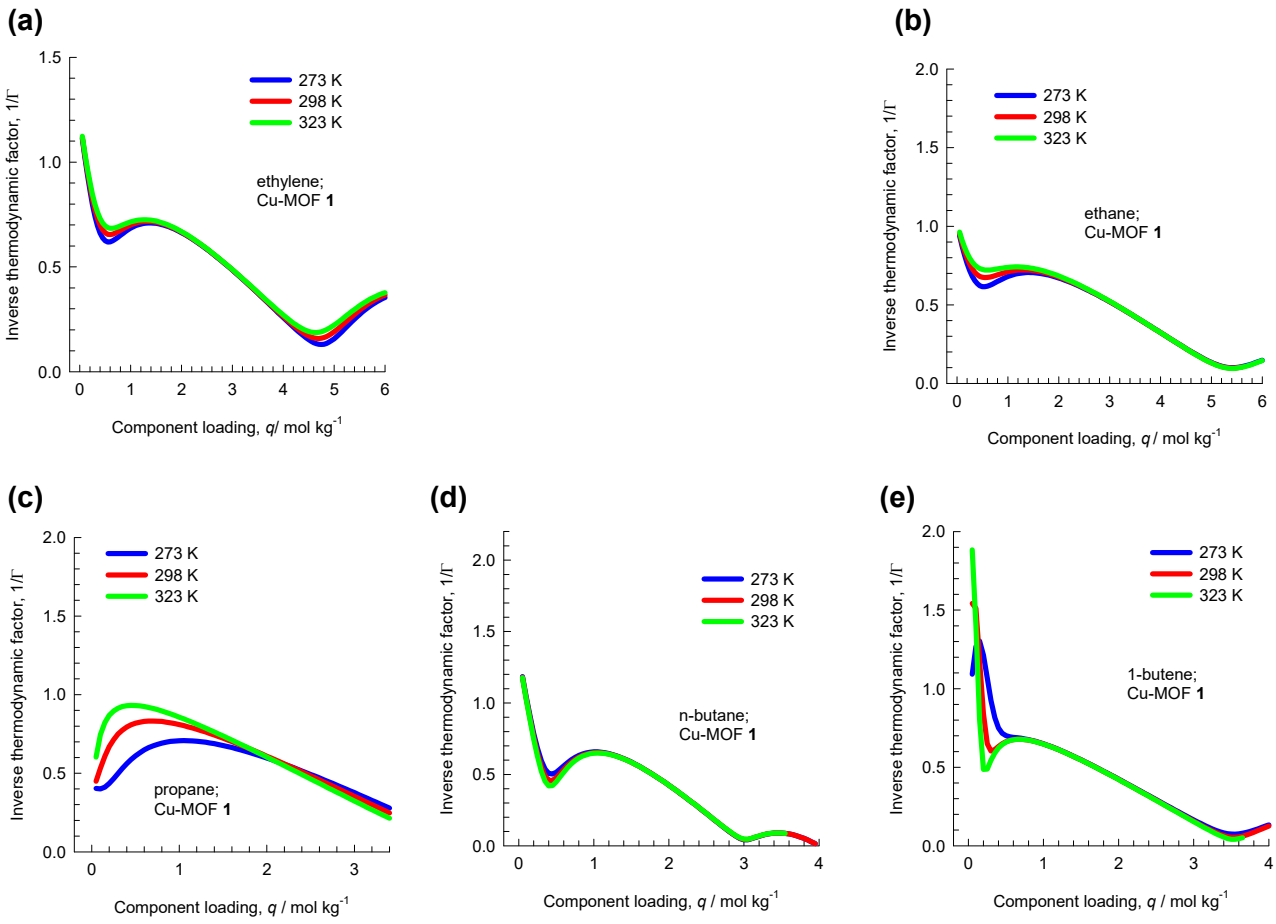

Fig. SM 3: Calculations of the inverse thermodynamic factor, $1/\Gamma$, as function of the component loading for (a) ethene, (b) ethane, (c) propane, (d) n-butane, and (e) 1-butene at 273 K, 298 K and 323 K in Cu-MOF **1**. These calculations are based on analytic differentiation of the 3-site Langmuir-Freundlich model fits of the adsorption branch for each guest molecule.

5. Isosteric heat of adsorption

The isosteric heat of adsorption, Q_{st}, defined as

$$Q_{st} = RT^2\left(\frac{\partial \ln p}{\partial T}\right)_q \tag{5}$$

was determined using the pure component isotherm fits using the Clausius-Clapeyron equation.

In Fig. SM 4, the values of Q_{st} for ethene, ethane, propane, n-butane, and 1-butene, calculated from using the fits of the adsorption branch (continuous solid lines) and desorption branches (dashed lines) of the isotherms are compared. For every guest molecule we see that the isotherm inflections leave strong imprints on the characteristics of the Q_{st} vs. q characteristics.

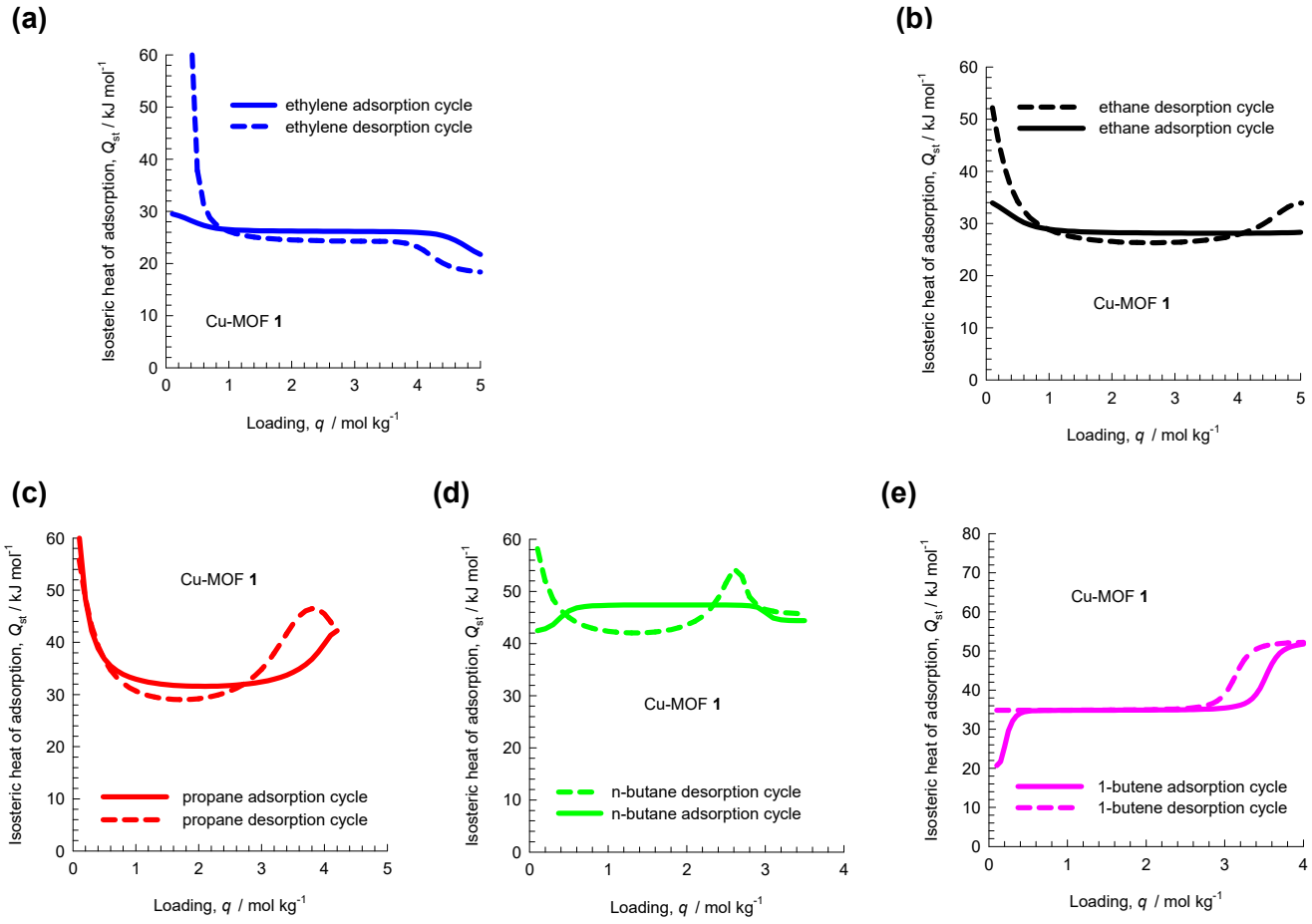

Fig. SM 4: Calculations of the isosteric heat of adsorption, Q_{st}, of (a) ethene, (b) ethane, (c) propane, (d) n-butane, and (e) 1-butene in Cu-MOF **1**. The continuous solid lines are the Q_{st} calculations using the fits of the adsorption branch of the unary isotherms. The dashed lines are the Q_{st} calculations using the fits of the desorption branch of the unary isotherms.

The inter-relation between isotherm inflections and the loading dependence of Q_{st} is best underscored in Fig. SM 5 that presents a comparison of the isosteric heat of adsorption, Q_{st}, of ethene, ethane, propane, n-butane, and 1-butene in Cu-MOF **1**; these Q_{st} calculations use the fits of the adsorption branch of the unary isotherms. In a loading range of about 1 – 3 mmol/g, the highest Q_{st} values are for n-butane; the hierarchy of Q_{st} values in this range is n-butane > 1-butene > propane > ethane > ethene.

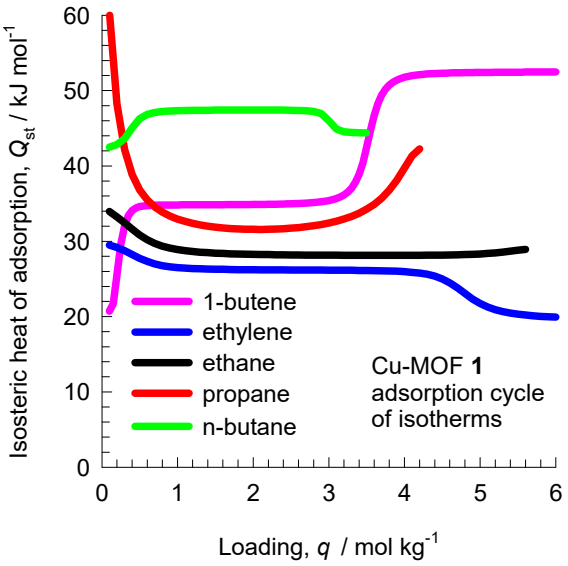

Fig. SM 5: Comparison of the isosteric heat of adsorption, Q_{st}, of ethene, ethane, propane, n-butane, and 1-butene in Cu-MOF **1**. The Q_{st} calculations use the fits of the adsorption branch of the unary isotherms.

Fig. SM 6 presents a comparison of Q_{st} vs. q with $1/\Gamma$ vs. q characteristics for (a) ethene, (b) ethane, (c) propane, (d) n-butane, and (e) 1-butene at 273 K, 298 K and 323 K in Cu-MOF **1**. It is quite apparent that the loading dependence of the isosteric heats of adsorption, Q_{st}, is intricately linked with the corresponding isotherm inflection characteristics. The two peaks in the Q_{st} vs. q data sets correspond with the corresponding troughs in the $1/\Gamma$ vs. q data.

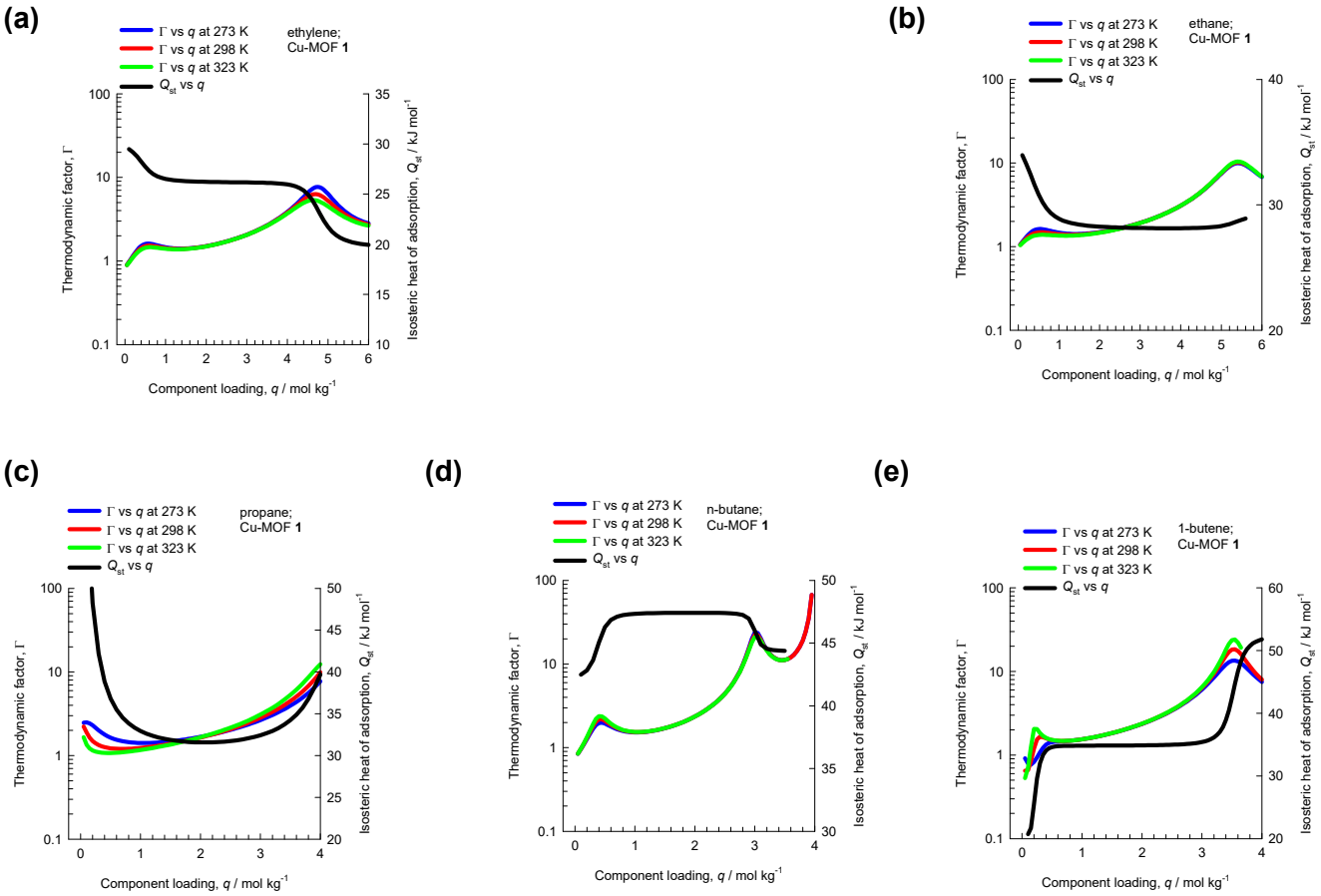

Fig. SM 6: Comparison of Q_{st} vs. q with $1/\Gamma$ vs. q characteristics for (a) ethene, (b) ethane, (c) propane, (d) n-butane, and (e) 1-butene at 273 K, 298 K and 323 K in Cu-MOF **1**.

6. IAST calculations of mixture adsorption

Fig. SM 7 presents the Ideal Adsorbed Solution Theory (IAST) calculations for component loadings for adsorption of equimolar ethene/ethane/propane/n-butane/1-butene gas mixtures in Cu-MOF **1** maintained at isothermal conditions at (a) 273 K, (b) 298 K, and (c) 323 K. We also note that component loadings are bunched into three fractions: C4-, C3- and C2-hydrocarbons. This indicates that ethene/ethane/propane/n-butane/1-butene gas mixtures can be separated into three fractions with different carbon numbers. At all three temperatures, n-butane is the most strongly adsorbed component.

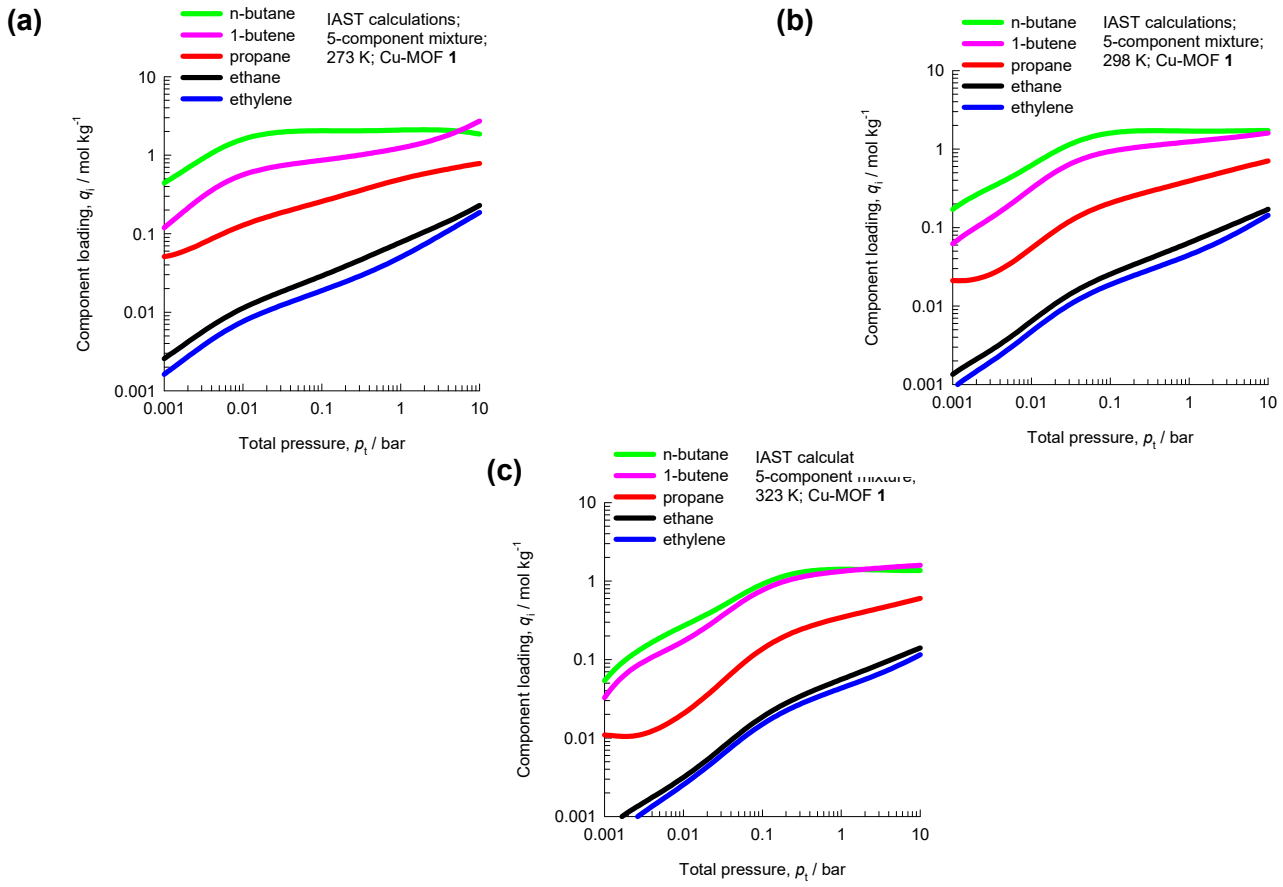

Fig. SM 7: IAST calculations for component loadings for adsorption of 5-component ethene/ethane/ propane/n-butane/1-butene gas mixtures in Cu-MOF **1** maintained at isothermal conditions at (a) 273 K, and (b) 298 K, and (c) 323 K. The IAST calculations are based on the isotherm fits using the adsorption branches of the isotherms.

The selectivity of preferential adsorption of component i over component j can be defined as

$$S_{ads} = \frac{q_i / q_j}{p_i / p_j} \tag{6}$$

In equation (6), q_i and q_j are the *absolute* component loadings of the adsorbed phase in the mixture.

In order to examine the feasibility of separation of ethane/ethene mixtures, Fig. SM 8 presents IAST calculations for adsorption selectivities of equimolar ethane/ethene gas mixtures in Cu-MOF **1** maintained at isothermal conditions at 273 K, 298 K, and 323 K. We note that the selectivities are only slightly above unity, and therefore effective separation of ethane/ethene mixtures with Cu-MOF **1** is not feasible.

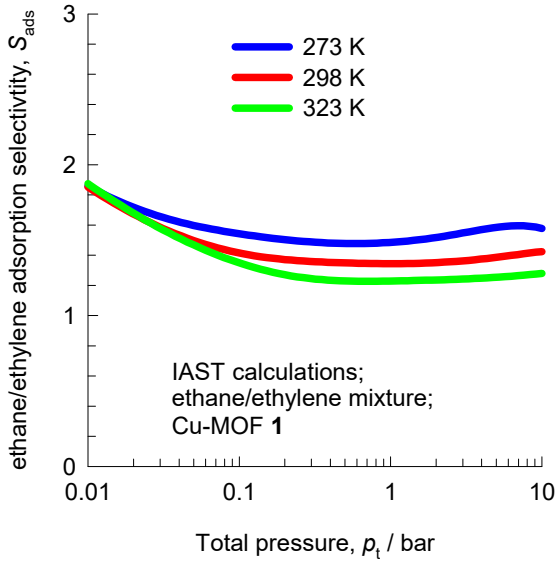

Fig. SM 8: IAST calculations for adsorption selectivities of equimolar ethane/ethene gas mixtures in Cu-MOF **1** maintained at isothermal conditions at 273 K, 298 K, and 323 K.

In order to examine the feasibility of n-butane/1-butene mixtures, Fig. SM 9 presents the IAST calculations for adsorption selectivities of equimolar n-butane/1-butene gas mixtures in Cu-MOF **1** maintained at isothermal conditions at 273 K, 298 K, and 323 K. We note that the S_{ads} values are higher at lower temperature. This suggests that the gate opening mechanism is more effective at lower temperatures for n-butane/1-butene separations.

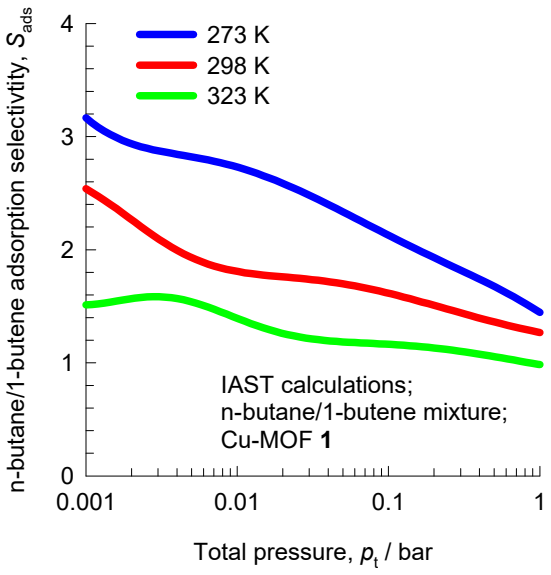

Fig. SM 9: IAST calculations for adsorption selectivities of equimolar n-butane/1-butene gas mixtures in Cu-MOF **1** maintained at isothermal conditions at 273 K, 298 K, and 323 K.

7. Transient breakthroughs in a fixed bed adsorber

Industrial separations of hydrocarbon mixtures are normally carried out in fixed bed adsorption devices. The performance of a fixed bed adsorber is dictated by a combination of adsorption selectivity and uptake capacity. To examine the separation potential of Cu-MOF **1**, we perform transient breakthrough simulations using the simulation methodology described in earlier work [3]. For all the simulations we choose: adsorber length, L = 0.3 m; superficial gas velocity in the bed, u = 0.04 m s^{-1}; voidage of the packed bed, ε = 0.4; crystal density, ρ = 1596 kg m^{-3}. For pulse chromatographic simulations, the pulse duration is taken as 10 s. For presenting the transient breakthrough simulation results, we use the

dimensionless time, $\tau = \frac{tu}{L\varepsilon}$, obtained by dividing the actual time, *t*, by the characteristic time, $\frac{L\varepsilon}{u}$.

Fig. SM 10a,b,c present simulations of transient breakthrough characteristics for 5-component ethene/ethane/propane/n-butane/1-butene gas mixtures in Cu-MOF **1** maintained at isothermal conditions at (a) 273 K, and (b) 298 K, and (c) 323 K. The partial pressure of each component in the inlet gas is 1 bar. At each temperature, the elution sequence is ethene, ethane, propane, 1-butene, and n-butane. For appreciation of the breakthroughs, a video animation of the transient traversal of the gas phase concentration fronts of each of the five guest molecules along the length of the fixed bed operating at 298 K has been uploaded as supplementary material. The breakthroughs suggest that the exit gas can be collected in three separate fractions with different C numbers, as indicated by the arrows in Fig. 10a,b,c. A close inspection of the breakthrough characteristics in Fig. 10 indicates that the C3/C4-separation appears to be more effective at 298 K and 323 K.

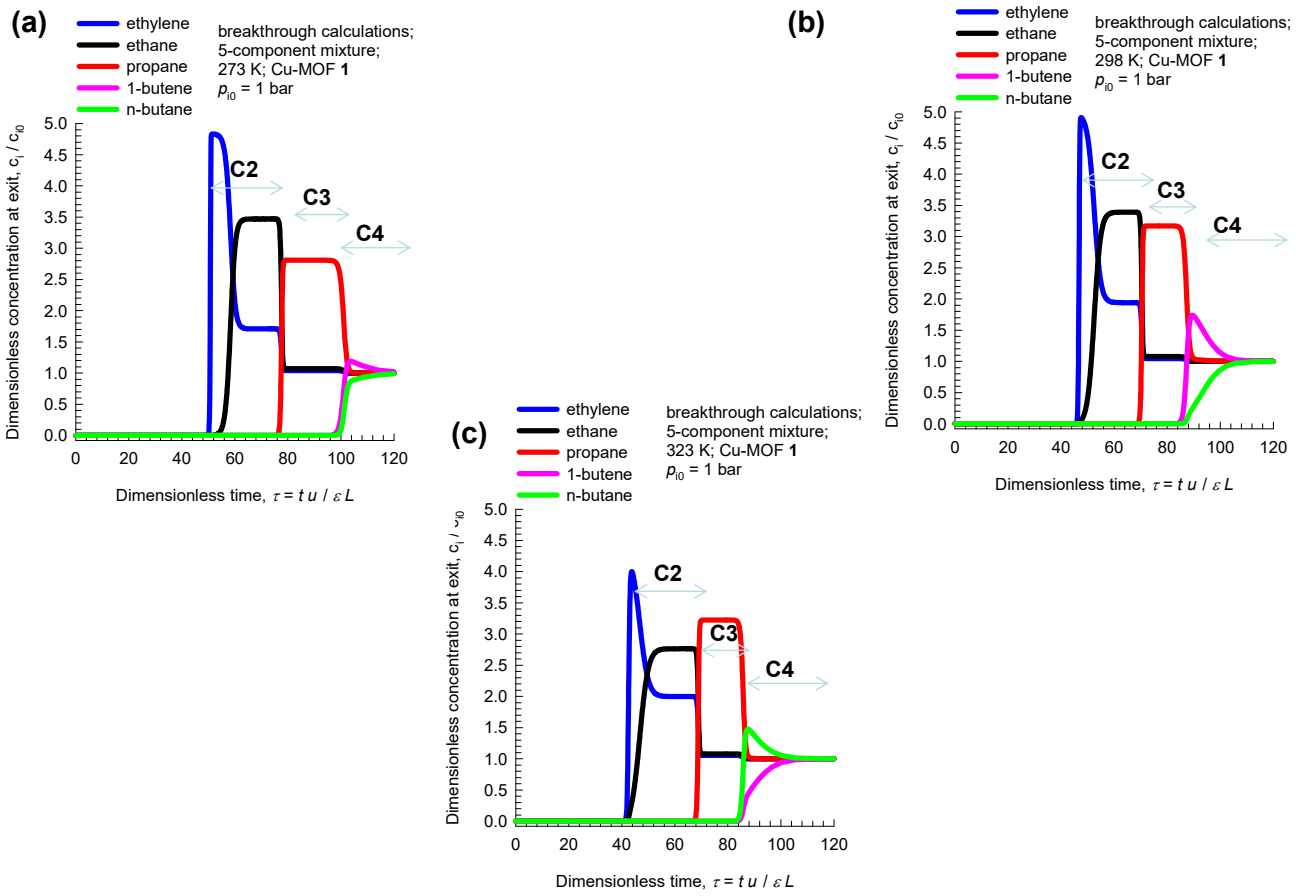

Fig. SM 10: Simulations of transient breakthrough characteristics for 5-component ethene/ethane/ propane/n-butane/1-butene gas mixtures gas mixtures in Cu-MOF **1** maintained at isothermal conditions at (a) 273 K, and (b) 298 K, and (c) 323 K. The partial pressure of each component in the inlet gas to the fixed bed is 1 bar. The breakthrough calculations are based on the isotherm fits using the adsorption branches of the isotherms.

The fractionation of C2/C3/C4 is best illustrated by the pulse chromatographic simulations performed at 298 K; see Fig. SM 11. The large time difference between the C3- and C4-peaks testifies to the effectiveness of C3/C4-separations at 298 K. The fractionation capability is best appreciated by viewing the video animations of the transient traversal of

the component peaks along the length of the fixed bed; these have been uploaded as Supplementary Material.

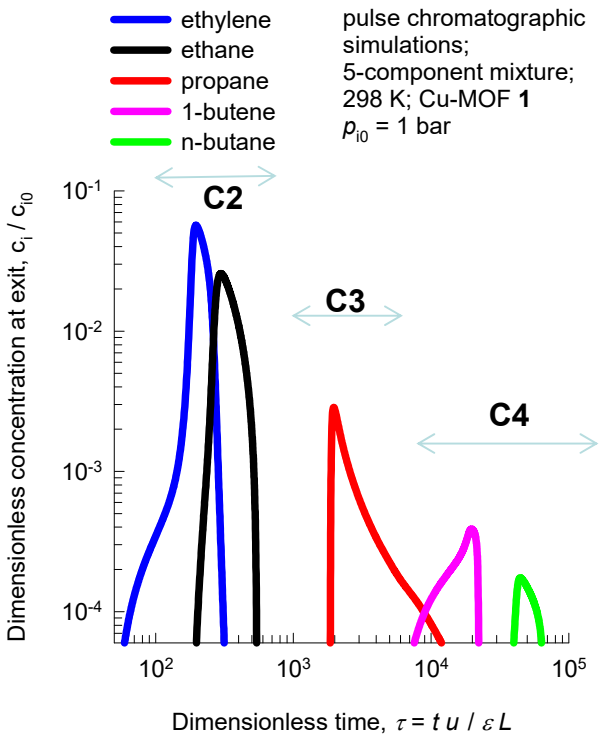

Fig. SM 11: Pulse chromatographic simulations for 5-component ethene/ethane/ propane/n-butane/1-butene gas mixtures gas mixtures in Cu-MOF **1** maintained at isothermal conditions at 298 K. The partial pressure of each component in the inlet gas to the fixed bed is 1 bar. The pulse injection time is 10 s. The breakthrough calculations are based on the isotherm fits using the adsorption branches of the isotherms.

In order to determine whether Cu-MOF **1** has the potential of separation of n-butane/1-butene mixtures, Fig. SM 12a,b,c presents the simulations of transient breakthrough characteristics for 2-component n-butane/1-butene gas mixtures in Cu-MOF **1** maintained at isothermal conditions at (a) 273 K, and (b) 298 K, and (c) 323 K. Only at the lowest temperature of 273 K is it possible to recover pure 1-butene in the gas phase.

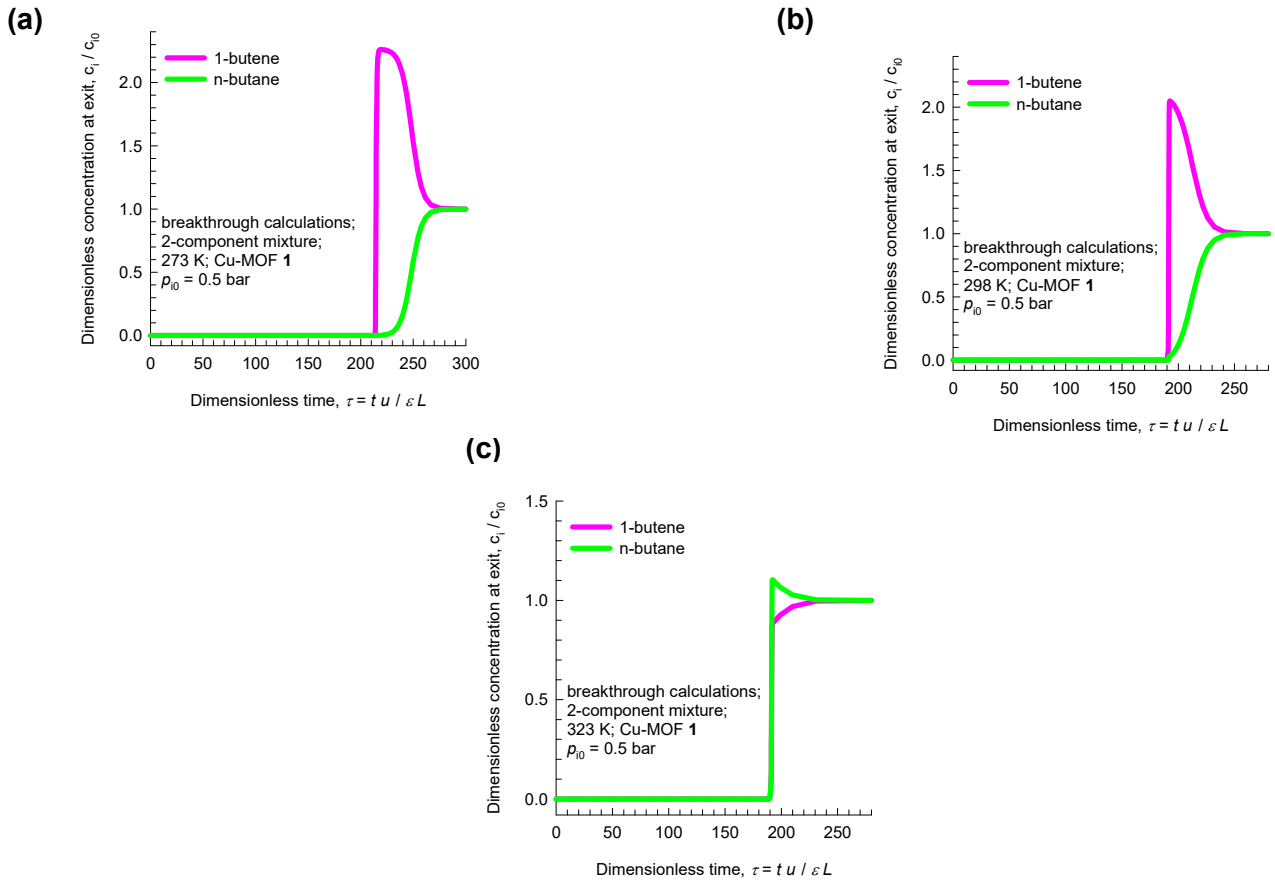

Fig. SM 12: Simulations of transient breakthrough characteristics for 2-component n-butane/1-butene gas mixtures in Cu-MOF **1** maintained at isothermal conditions at (a) 273 K, and (b) 298 K, and (c) 323 K. The partial pressure of each component in the inlet gas to the fixed bed is 0.5 bar. The breakthrough calculations are based on the isotherm fits using the adsorption branches of the isotherms.

8. Notation

b_A	Langmuir-Freundlich constant for adsorption site A, $Pa^{-\nu_{iA}}$
b_B	Langmuir-Freundlich constant for adsorption site B, $Pa^{-\nu_{iB}}$
b_C	Langmuir-Freundlich constant for adsorption site C, $Pa^{-\nu_{C}}$
c_i	molar concentration of species *i* in gas mixture, mol m^{-3}
c_{i0}	molar concentration of species *i* in gas mixture at inlet to adsorber, mol m^{-3}
E_A	energy parameter, J mol^{-1}
E_B	energy parameter, J mol^{-1}
E_C	energy parameter, J mol^{-1}
L	length of packed bed adsorber, m
p_i	partial pressure of species *i* in mixture, Pa
p_t	total system pressure, Pa
q_i	component molar loading of species *i*, mol kg^{-1}
$q_{i,sat}$	molar loading of species *i* at saturation, mol kg^{-1}
Q_{st}	isosteric heat of adsorption, J mol^{-1}
R	gas constant, 8.314 J mol^{-1} K^{-1}
S_{ads}	adsorption selectivity, dimensionless
t	time, s
T	absolute temperature, K
u	superficial gas velocity in packed bed, m s^{-1}
V_{pore}	pore volume, m^3 kg^{-1}
Z	Compressibility factor, dimensionless

Greek letters

Γ	thermodynamic factor, dimensionless
ε	voidage of packed bed, dimensionless

ν_A	Freundlich exponent for site A, dimensionless
ν_B	Freundlich exponent for site B, dimensionless
ν_C	Freundlich exponent for site C, dimensionless
ρ	framework density, kg m^{-3}
τ	time, dimensionless

Subscripts

i	referring to component *i*
A	referring to site A
B	referring to site B
C	referring to site C
sat	referring to saturation conditions
t	referring to mixture

Superscripts

excess	referring to excess loading

9. References

[1] E.D. Bloch, W.L. Queen, R. Krishna, J.M. Zadrozny, C.M. Brown, J.R. Long, Science 335 (2012) 1606-1610.

[2] Y. He, W. Zhou, R. Krishna, B. Chen, Chem. Commun. 48 (2012) 11813-11831.

[3] R. Krishna, RSC Adv. 5 (2015) 52269-52295.

[4] R. Krishna, Phys. Chem. Chem. Phys. 17 (2015) 39-59.

[5] Y. He, R. Krishna, B. Chen, Energy Environ. Sci. 5 (2012) 9107-9120.

[6] T.-L. Hu, H. Wang, B. Li, R. Krishna, H. Wu, W. Zhou, Y. Zhao, Y. Han, X. Wang, W. Zhu, Z. Yao, S.C. Xiang, B. Chen, Nat. Commun. 6 (2015) 7328. (http://dx.doi.org/doi:10.1038/ncomms8328)

[7] M.C. Das, Q. Guo, Y. He, J. Kim, C.G. Zhao, K. Hong, S. Xiang, Z. Zhang, K.M. Thomas, R. Krishna, B. Chen, J. Am. Chem. Soc. 134 (2012) 8703-8710.

[8] H.-M. Wen, B. Li, H. Wang, C. Wu, K. Alfooty, R. Krishna, B. Chen, Chem. Commun. 51 (2015) 5610-5613.

[9] S. Yang, A.J. Ramirez-Cuesta, R. Newby, V. Garcia-Sakai, P. Manuel, S.K. Callear, S.I. Campbell, C.C. Tang, M. Schröder, Nature Chemistry 7 (2014) 121-129.

[10] B. Li, Y. Zhang, R. Krishna, K. Yao, Y. Han, Z. Wu, D. Ma, Z. Shi, T. Pham, B. Space, J. Liu, P.K. Thallapally, J. Liu, M. Chrzanowski, S. Ma, J. Am. Chem. Soc. 136 (2014) 8654-8660.

[11] Y. Zhang, B. Li, R. Krishna, Z. Wu, D. Ma, Z. Shi, T. Pham, K. Forrest, B. Space, S. Ma, Chem. Commun. 51 (2015) 2714-2717.

[12] D.-L. Chen, N. Wang, C. Xu, G. Tu, W. Zhu, R. Krishna, Micropor. Mesopor. Mater. 208 (2015) 55-65.

[13] P. Li, Y. He, H.D. Arman, R. Krishna, L. Weng, B. Chen, Chem. Commun. 50 (2014) 13081-13084.

[14] D.-L. Chen, H. Shang, W. Zhu, R. Krishna, Chem. Eng. Sci. 117 (2014) 407-415.

[15] J. Duan, W. Jin, R. Krishna, Inorg. Chem. 54 (2015) 4279-4284.

[16] Y. He, C. Song, Y. Ling, C. Wu, R. Krishna, B. Chen, APL Mater. 2 (2014) 124102.

[17] J. Jia, L. Wang, F. Sun, X. Jing, Z. Bian, K. Cai, L. Gao, R. Krishna, G.S. Zhu, Chem. Eur. J. 20 (2014) 9073-9080.

[18] M. Hartmann, S. Kunz, D. Himsl, O. Tangermann, S. Ernst, A. Wagener, Langmuir 24 (2008) 8634-8642.